Journal of Molecular Structure 1048 (2013) 464–470

Contents lists available at SciVerse ScienceDirect

Journal of Molecular Structure

journal homepage: www.elsevier.com/locate/molstruc

# Spectroscopic and computational study of a new isomer of salinomycin

Radosław Pankiewicz *

*Faculty of Chemistry, Adam Mickiewicz University in Poznań, Umultowska 89b, PL-61-614 Poznań, Poland*

## HIGHLIGHTS

- I have synthesized a new derivative of salinomycin.
- The new isomer was fully characterized by multinuclear 2D NMR, NOESY and MALDI-TOF.
- The properties of the new compound were additionally study by semiempirical (PM5) and DFT (B3LYP).
- A potential mechanism of the rearrangement was proposed.

## ARTICLE INFO

*Article history:*
Received 29 April 2013
Received in revised form 10 June 2013
Accepted 10 June 2013
Available online 14 June 2013

*Keywords:*
Salinomycin
Rearrangement
NMR
PM5
DFT

## ABSTRACT

A new derivative of polyether ionophore salinomycin was obtained as a result of a rearrangement catalysed by sulphuric acid in two-phase medium of water/methylene chloride solution. The new isomer was fully characterized by multinuclear 2D NMR, NOESY and MALDI-TOF. The properties of the new compound were additionally study by semiempirical (PM5) and DFT (B3LYP) methods. A potential mechanism of the rearrangement was also proposed.



## 1. Introduction

Polyether ionophores make a wide class of natural and synthetic compounds. They are used to control ketosis and bloat in cattle and are applied as growth promoting feed additives to cattle and sheep. They have been widely used as a coccydiostatic in rearing of cattle and poultry [1]. Coccydiostatics are a group of chemotherapeutic substances that can be administered to animals, mainly to poultry, for prophylactic purposes or treatment of coccidiosis caused by protozoa *Eimeria* [2–6]. The main feature of this group is the ability to complex ions and transport them through the natural and synthetic membranes. Ionophores are host molecules that bind ionic guests and transport them across a membrane such as a bulk organic phase or a phospholipid bilayer like e.g. the ones present in a cell or subcellular organelle. Ionophores can transport and hence regulate the concentrations of the main biological cations such as $Li^+$, $Na^+$, $K^+$, $Ca^{2+}$ [7,8], heavy metal cations $Pb^{2+}$, $Cd^{2+}$ [9] and some anions ($Cl^-$) or neutral molecules ($NH_3$). These antibiotics are effective against gram-positive bacteria, mycobacteria and fungi [10]. One of them, Salinomycin isolated from *Streptomyces albus* like other ionophores, is able to dynamically adapt to the cation with which it is to make a complex [9,11,12]. However, thanks to the ability to make a pseudo-ring, like many ionophores, on complexation it prefers closing the best geometrically fitted cation in the pseudo-ring. The complexes with $K^+$ ions it forms are four orders of magnitude more stable than those it makes with $Na^+$ cations. These features are useful for molecular recognition and make basis for development of ion receptors and ion-selective electrodes.

## 2. Results and discussion

Salinomycin acid (SalH) was synthesised from its sodium salt (SalNa) according to the following method.

In order to obtain SalH the methylene chloride solutions of SalNa were shaken with water solutions of $H_2SO_4$ of different pH. The most effective conversion was observed for the solutions of pH 2. The effectiveness of this process was controlled by HPLC equipped, additionally, with Corona detector, because SalH similarly as SalNa has insignificant absorption in UV–Vis range. For more concentrated sulphuric acid solutions the chromatograms of the products revealed an extra signal with a significantly shorter retention time

* Tel.: +48 618291553.
*E-mail address:* radek@px.pl

0022-2860/$ - see front matter © 2013 Elsevier B.V. All rights reserved.
http://dx.doi.org/10.1016/j.molstruc.2013.06.020

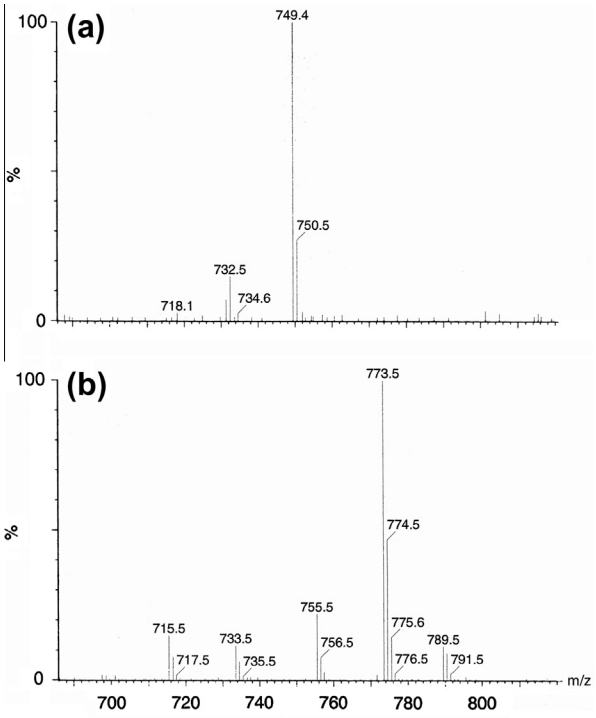


**Fig. 1.** MALDI MS spectra in negative (a) and positive (b) ion detection mode of SalX.

(3.8 min versus 6.3 min for SalNa and 5.8 min for SalH). Preliminary I assumed that this signal can be assigned to a decomposition product of salinomycin. Although salinomycin is known not to absorb in the UV–Vis range, which was the reason for the use of a Corona detector, all the time standard UV–Vis detector was on. That is why it was established that the new chemical compound absorbs in the UV range with a maximum absorption at $\lambda = 217$ nm. The synthesised compound collected with the leak from the chromatographic column was subjected to MS analysis. The MS spectra showed signals of a molecular ion at $m/z = 773.5$ in positive and $m/z = 749.4$ in negative ion detection mode. These $m/z$ values are the same as in the MS spectra of salinomycin acid (with complexed $Na^+$ in positive ion mode) (Fig. 1). Analysis of the data collected has shown that the new compound is a new isomer of salinomycin (SalX) showing less affinity to the stationary phase of C18 chromatographic column. Additionally the UV absorption suggested the existence of conjugated double bonds.

After this observation the synthesis procedure was optimized to obtain SalX in good yield. The use of $H_2SO_4$ solution of pH 1 after 12 h of stirring gave the isomer with 94% yield (separated by HPLC). The isomer was stable and did not undergo further transformations (see Scheme 1.)

In order to identify the structure of the isomer it was subjected to NMR study. To obtain full assignments of $^1H$ and $^{13}C$, the 2D NMR techniques, $^1H$–$^1H$ COSY, $^1H$–$^{13}C$ HSQC and $^1H$–$^{13}C$ HMBC were used. The data are given in Table 1, the $^1H$–$^{13}C$ HSQC spectrum with the assignments of NMR cross peaks are given in Fig. 2.

Most of the $^1H$ and $^{13}C$ assignments are in agreement with those given in literature [9,13,14], but some of them showed significant differences [C(16)—C(22)] and [H(14)—H(16), H(18)—H(20), H(22), H(23)], which indicated clearly that the isomerization process had caused a rearrangement of the spiro rings in the central region of the molecule. Very significant changes in the chemical shift of C(17) from ~100.3 to 160.4 ppm and C(21) from ~107.7 to 177.4 ppm and a signal of H(20) at low fields was the evidence of opening of two spiro rings. Significant changes in chemical shifts were also observed for C(18), C(19), C(20), C(22) and H(18), H(19), H(22), H(23). Similar ring openings were observed for a different salinomycin isomer obtained in a different way [14]. The authors of this paper reported the rearrangements of spiro rings to a furan moiety. In this work a structure with two coupled double bonds was found to form but no evidence in the HMBC spectra of a long-range correlation of H(20) and C(21) was detected. Instead, a long-range correlation between H(20) and C(24) was observed. Only a weak shift of C(24) signal suggest that it is still bonded to the ether oxygen atom. Additionally the signal assigned to H(20) is still observed but significantly shifted towards weaker field, from ~4.04 ppm to 7.29 ppm. All these facts testify to the formation of a new structure which contains a ten-membered lactone ring as the main element. The structure of this new isomer is given in Scheme 2.

Signals assignment to H and C atoms from other parts of SalX molecule have shifts nearly identical to the analogous resonances in salinomycin, strongly suggesting that this part of molecule is unaltered in isomer.

The theoretical $^1H$ and $^{13}C$ NMR spectra were also computed using DFT methods. All data obtained (Table 1) were in very good agreement with experimental values. The correlation coefficient was $R^2 = 0.99$ for $^{13}C$ and $R^2 = 0.93$ for $^1H$ NMR.

To visualize the structure of the new salinomycin derivative and to analyse the conformation of the molecular chain, the DFT calculation was performed using GAUSSIAN 03 package. The calculated 3D structure is given in Fig. 3.

SalX has a pseudo-cyclic structure which is formed thanks to the appearance of a hydrogen bond of head-to-tail type between the carboxyl group and the hydroxyl group attached to the last

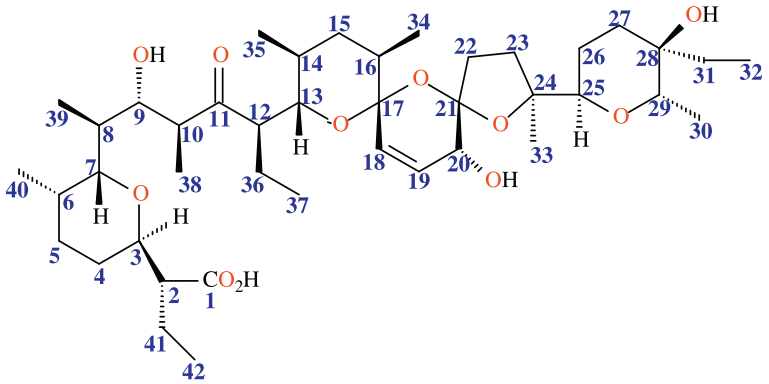


**Scheme 1.** Salinomycin (SalH).

**Table 1**
$^{1}$H NMR and $^{13}$C NMR chemical shifts.

| No. atom | $\delta_H$ and $\delta_C$ (ppm) | | | |
|---|---|---|---|---|
| | H | C | Calculated H | Calculated C |
| 1 | – | 178.4 | – | 187.19 |
| 2 | 2.91 (ddd) 1H<br>$^{3}J_{H2,H14a}$ = 14.8<br>$^{3}J_{H2,H3}$ = 10.8<br>$^{3}J_{H2,H14b}$ = 3.6 | 49.1 | 2.43 | 60.06 |
| 3 | 3.99 (dd) 1H<br>$^{3}J_{H3,H4}$ = 6.0 | 75.0 | 4.23 | 70.06 |
| 4a | 1.39* (m) 1H | 19.7 | 1.21 | 34.82 |
| 4b | 1.95* (m) 1H | | 1.83 | |
| 5a | 1.80* (m) 1H | 26.2 | 2.18 | 30.42 |
| 5b | 1.48* (m) 1H | | 1.50 | |
| 6 | 1.81* (m) 1H | 28.0 | 2.17 | 41.74 |
| 7 | 3.58 (dd) 1H<br>$^{3}J_{H6,H7}$ = 10.0<br>$^{3}J_{H7,H8}$ = 1.5 | 71.5 | 3.60 | 82.60 |
| 8 | 1.47* (m) 1H | 36.5 | 2.90 | 53.40 |
| 9 | 4.09 (d) 1H<br>$^{3}J_{H9,H10}$ = 7.0 | 70.3 | 3.40 | 82.28 |
| 10 | 2.94* (m) 1H | 47.5 | 3.20 | 58.22 |
| 11 | – | 218.6 | – | 233.67 |
| 12 | 2.63 (dt) 1H<br>$^{3}J_{H12,H13}$ = 10.5<br>$^{3}J_{H12,H36}$ = 2.3 | 58.0 | 3.01 | 64.59 |
| 13 | 3.78 (dd) 1H<br>$^{3}J_{H12,H13}$ = 1.2<br>$^{3}J_{H13,H14}$ = 9.5 | 74.1 | 3.56 | 82.78 |
| 14 | 1.57* (m) 1H | 33.6 | 2.43 | 38.77 |
| 15a | 2.24 (ddd) 1H<br>$^{2}J_{H15a,H15b}$ = 13.7<br>$^{3}J_{H15,H14}$ = 10.9<br>$^{3}J_{H13,H14}$ = 2.7 | 39.9 | 2.21 | 45.55 |
| 15b | 1.25* (m) 1H | | 1.73 | |
| 16 | 2.98* (m) 1H | 30.9 | 3.35 | 42.22 |
| 17 | – | 160.4 | | 165.14 |
| 18 | 6.03 (d) 1H<br>$^{3}J_{H17,H18}$ = 3.0 | 103.7 | 5.23 | 119.45 |
| 19 | 6.26 (dd) 1H<br>$^{3}J_{H19,H20}$ = 1.8 | 109.8 | 4.61 | 102.97 |
| 20 | 7.29 (d) 1H | 140.3 | 6.63 | 150.85 |
| 21 | – | 177.4 | | 187.58 |
| 22a | 2.69 (ddd) 1H<br>$^{2}J_{H22a,H22b}$ = 17.9<br>$^{3}J_{H22a,H23a}$ = 10.5<br>$^{3}J_{H22a,H23b}$ = 6.5 | 29.6 | 2.54 | 34.83 |
| 22b | 2.50 (ddd) 1H<br>$^{3}J_{H22b,H23a}$ = 10.5<br>$^{3}J_{H22b,H23b}$ = 2.1 | | 2.09 | |
| 23a | 2.42 (ddd) 1H<br>$^{2}J_{H23a,H23b}$ = 12.9 | 29.2 | 2.60 | 40.49 |
| 23b | 1.85* (m) 1H | | 1.24 | |
| 24 | – | 87.3 | | 88.44 |
| 25 | 3.64 (dd) 1H<br>$^{3}J_{H25,H26a}$ = 11.3<br>$^{3}J_{H25,H26b}$ = 2.1 | 73.2 | 3.48 | 79.42 |
| 26a | 1.66* (m) 1H | 21.3 | 2.08 | 24.02 |
| 26b | 1.50* (m) 1H | | 1.48 | |
| 27a | 1.70* (m) 1H | 29.1 | 2.14 | 31.33 |
| 27b | 1.65* (m) 1H | | 1.39 | |
| 28 | – | 71.4 | | 78.31 |
| 29 | 3.84 (q) 1H<br>$^{3}J_{H29,H30}$ = 6.8 | 76.7 | 3.96 | 87.00 |
| 30 | 1.22 (d) 3H | 14.3 | 1.09 | 16.48 |
| 31 | 1.37 (m) 2H | 30.8 | 1.34 | 36.26 |
| 32 | 0.92 (t) 3H<br>$^{3}J_{H31,H32}$ = 7.5 | 6.3 | 0.98 | 8.43 |
| 33 | 1.34 (s) 3H | 22.9 | 1.48 | 21.48 |
| 34 | 1.23* (d) 3H<br>$^{3}J_{H16,H34}$ = 7.5 | 21.2 | 1.17 | 19.03 |
| 35 | 0.82 (d) 3H<br>$^{3}J_{H14,H36}$ = 6.7 | 12.8* | 1.06 | 24.23 |
| 36a | 1.75* (m) 1H | 15.4 | 1.90 | 28.29 |
| 36b | 1.80* (m) 1H | | 2.04 | |
| 37 | 0.76* (t) 3H | 12.8* | 1.03 | 16.06 |

**Table 1** (*continued*)

| No. atom | $\delta_H$ and $\delta_C$ (ppm) | | | |
|---|---|---|---|---|
| | H | C | Calculated H | Calculated C |
| 38 | 0.85 (d) 3H<br>$^3J_{H10,H38}$ = 7.0 | 13.3 | 1.08 | 19.71 |
| 39 | 0.75* (d) 3H<br>$^3J_{H8,H39}$ = 6.8 | 7.0 | 1.40 | 19.16 |
| 40 | 0.94* (d) 3H<br>$^3J_{H6,H40}$ = 6.8 | 10.8 | 1.10 | 19.70 |
| 41a | 1.37* (m) 1H | 22.5 | 1.75 | 28.33 |
| 41b | 1.53* (m) 1H | | 1.85 | |
| 42 | 0.95* (dd) 3H<br>$^3J_{H41a,H42}$ = 7.2<br>$^3J_{H41b,H42}$ = 9.8 | 11.9 | 0.91 | 10.37 |
| 1-OH | Not observed | – | 8.36 | – |
| 9-OH | 2.9* (bs) | – | 2.22 | – |
| 13-OH | 1.9* (bs) | – | 1.80 | – |
| 28-OH | Not observed | – | 3.28 | – |

Correlations – calculated to the measured chemical shifts: $^{13}C$ $R^2$ = 0.99, $^1H$ $R^2$ = 0.93, *approximate value.

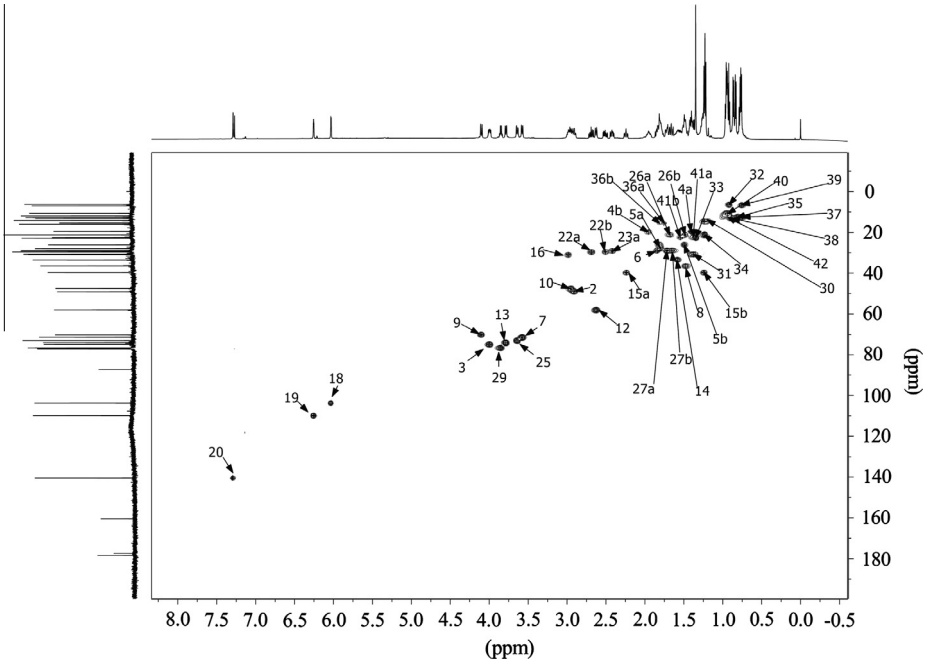


**Fig. 2.** The $^1H$–$^{13}C$ HSQC spectrum with the assignments of NMR cross peaks.

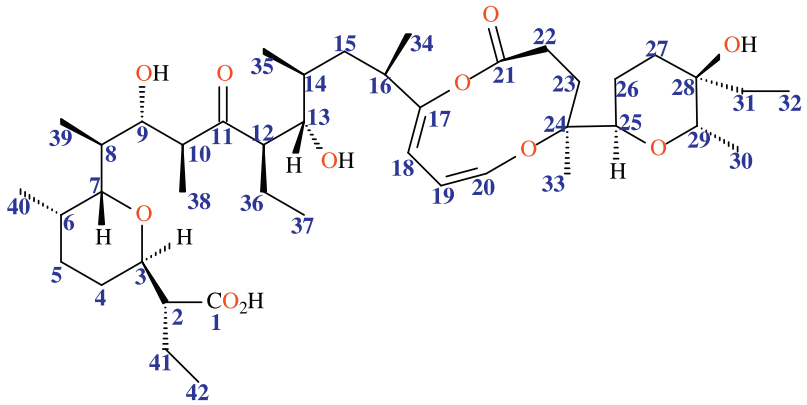

**Scheme 2.** Newly obtained salinomycin derivative (SalX).

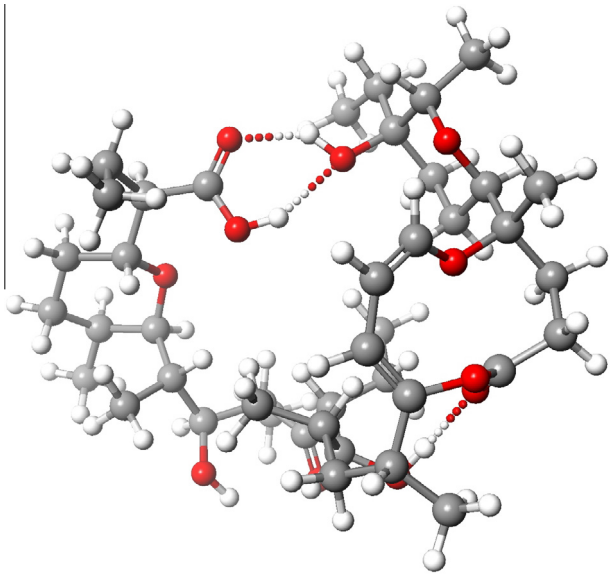

**Fig. 3.** Calculated structure (B3LYP) of salinomycin derivative (SalX).

pyrane ring, just as in salinomycin sodium salt [15]. The structure is also stabilised by one intramolecular hydrogen bond between O(37)H group and C(21)=O group from the new ten-membered ring. The hydrogen bond length is 2.74 Å with the bond angle 170.7°. The molecular chain is folded and makes a pseudo-loop, so that consequently H(20) is neighboring H(35). To confirm these conclusions the NOESY spectrum ($^1$H–$^1$H) was measured. The contacts are collected in Table 2.

The most important correlations for understanding of the conformation of this molecule are between H(18) and H(14), H(35) and also between H(25a,b) and H(33). These data determine the conformation of the rearranged part of the isomer. Moreover, analysis of the NOESY spectrum permits indirect determination of stereochemistry of C(24) atom. The protons from the methyl group H(33) joined to C(24) are in contact with H(25) and H(30) groups, on the other hand, proton H(18) is in contact with H(14), H(15), H(16) and H(35). Such simultaneous contacts would not be possible if the configuration of C(24) was *R* instead of the postulated one – S. The conclusion obtained from NOESY ($^1$H–$^1$H) measurement fully confirmed theoretical computations.

SalX in this conformation has not all hydrophilic group directed to the centre of the molecule. This structure is expected to have worse complexating abilities than salinomycin. To verify this hypothesis, the semiempirical computation (PM5) of heats of complexation was performed. The data obtained are collected in Table 3.

The heat of complexation is (HOF (heat of formation) of a complex) – (HOF of isolated ligand + HOF of isolated cation). The lower the heat of complexation the more preferred the complex. The heats of complexation (HOC) for complexes of SalX with all cations studied ($Li^+$, $Na^+$ and $K^+$) take higher values than the respective complexes with salinomycin, which is in agreement with the hypothesis proposed. Additionally, for SalX the most preferred is the complex with $Na^+$ cation in contrast to salinomycin whose preferred complex is with $K^+$ cation, which means that $Na^+$ cation fits better the cavity of the isomer molecule.

SalX was obtained as a result of a rearrangement of salinomycin in a strong acidic solution. It is obvious that the first step of this rearrangement was protonation of the one of oxygen atoms. A key issue to propose this mechanism was to establish which atom was protonated. To resolve this problem the most likely protonated structures were calculated by DFT method. The data are collected in Table 4.

On the basis of the calculations three structures were proposed, protonated at different oxygen atoms O(13), O(17) and O(21). The lowest energy was found for the structure with a proton attached to O(13). At this position proton is additionally stabilised by the electron pair from the carbonyl carbon atom O(11). The site of protonation and the conformation of the molecule prior to rearrangement are shown in Fig. 4.

Most probably the rearrangement starts from protonation of O(13) and then involves the tertiary carbocation stabilised by the oxygen atom O(17) and ends with a nucleophilic attack of the electron pair from O(20) on C(24) which is engaged in the bond closing the new ten-membered ring (Scheme 3.).

**Table 2**
The most important NOESY ($^1$H–$^1$H) contacts.

| Atom no | Contacts | | | |
|---|---|---|---|---|
| H7 | H9 | | | |
| H10 | H12 | | | |
| H15a | H18 | H35 | | |
| H18 | H14 | H15 | H16 | H35 |
| H22a | H33 | | | |
| H22b | H33 | | | |
| H25 | H30 | H33 | | |

**Table 3**
Calculated by PM5 heats of complexation [kJ/mol].

| Cation | dHOF of salinomycin | dHOF of SalX |
|---|---|---|
| Li | −627.68 | −548.52 |
| Na | −659.74 | −634.08 |
| K | −676.23 | −594.38 |

**Table 4**
Calculated by B3LYP energy of protonated SalX (hartree [a.u.]).

| No of protonated atom | Energy of protonated molecule [a.u.] |
|---|---|
| O13 | −2470.9910 |
| O17 | −2470.8674 |
| O21 | −2470.9023 |

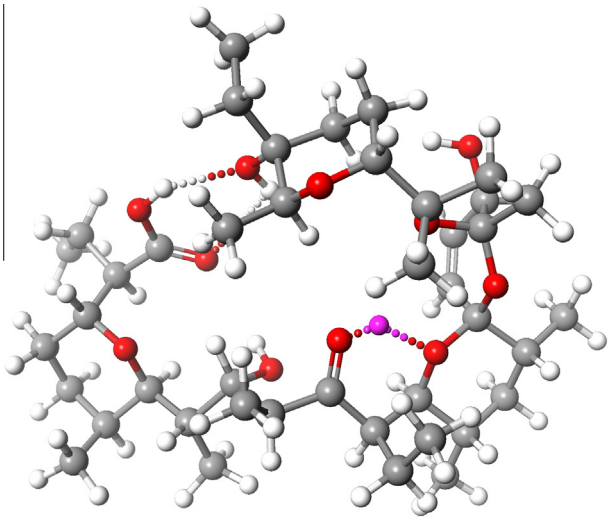

**Fig. 4.** Calculated structure (B3LYP) of protonated salinomycin.

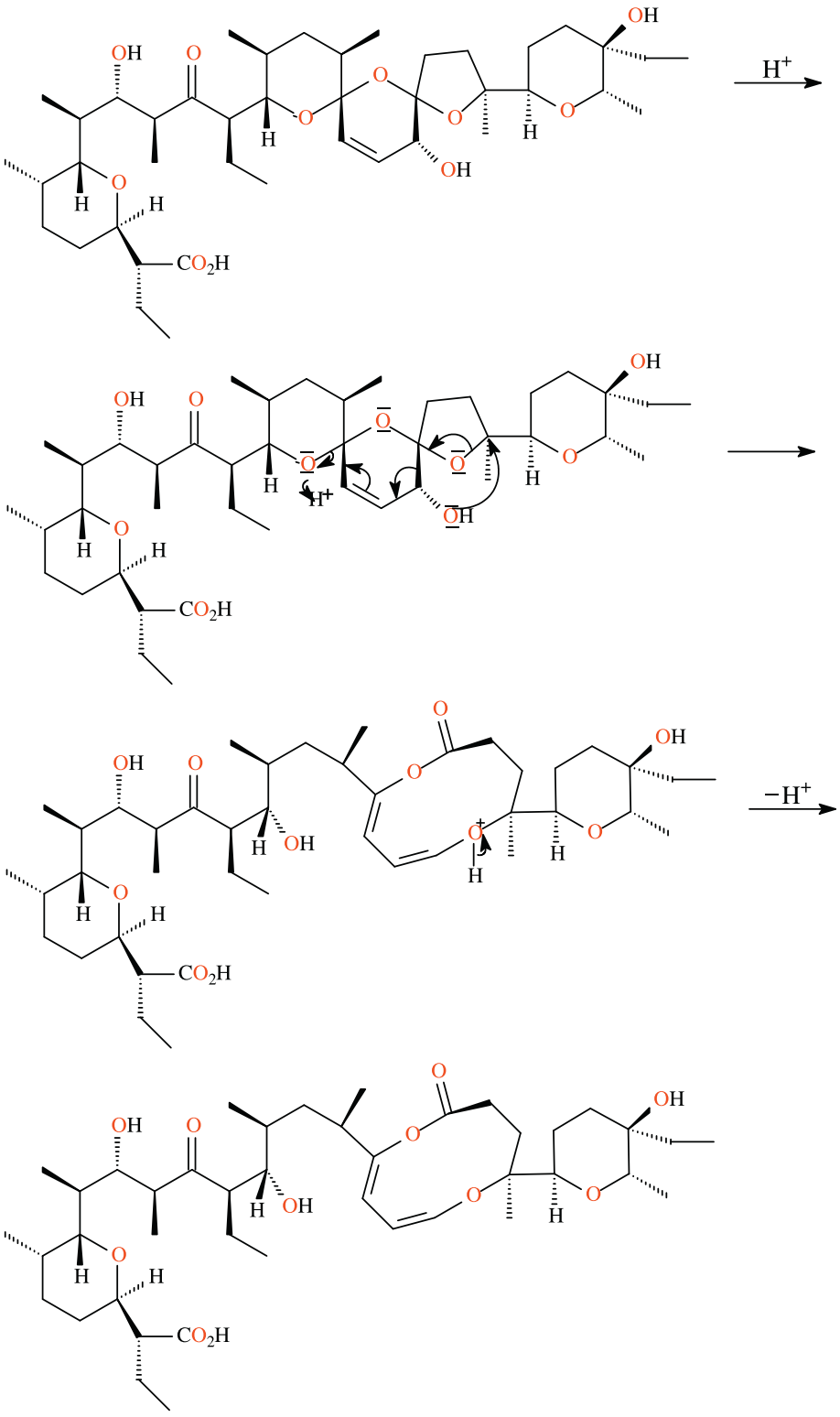

**Scheme 3.** Proposed mechanism of rearrangement.

## 3. Experimental section

### 3.1. The synthesis of salinomycin derivative (SalX)

The commercially available salinomycin sodium salt (250 mg) was dissolved in 30 mL $CH_2Cl_2$. The organic solution was then poured together with aqueous solution of $H_2SO_4$ (2 mL $H_2SO_4$ in 60 mL $H_2O$) and vigorously stirred for 12 h. The reaction progress was monitored by HPLC analysis. The organic phase was isolated and extracted with portions of water to obtain pH near neutral. After that $CH_2Cl_2$ solution was evaporated under reduced pressure to obtain oily residue.

### 3.2. Elementary analysis

The elementary analysis was carried out on Perkin Elmer CHN 240. For the salinomycin derivative (SalX) ($C_{43}H_{72}O_{10}$) (calculated: C 68.95% H 9.69%, found: C 68.81%; H 9.45%).

### 3.3. HPLC measurement

HPLC separations were obtained in a Dionex ASI-100 equipped with a P680 HPLC pump using Thermo Hypersil GOLD 150 × 4.6 column and as well as a Dionex PDA-100 Photodiode Array Detector. The flow rate was 2 ml/min with injection volumes of about 20 μL. As the mobile phase, we used mixtures of acetonitrile and water in various ratios depending on particular separation and changed during analysis from 70:30 to 80:20 acetonitrile/water. The analytical wavelength was 217 nm. To detect nonvolatile analyte, without a chromophore, a Corona® ESA Inc. detector was used.

### 3.4. MALDI measurement

In my report the mass of molecular ion was determined by MALDI-TOF tandem MS in positive and negative ion detection mode. The MALDI-TOF spectra were obtained on a Water/Micromass (Manchester, UK) Q-TOF Premier mass spectrometer (software MassLynx V4.1, Manchester, UK) fitted with a 200 Hz repetition rate Nd/YAG laser ($\lambda$ = 355 nm, power density 107 W/cm$^2$). The compounds analysed were solids and the matrix used was DHB.

### 3.5. NMR measurement

The NMR spectra of SalX (0.05 mol L1) were recorded at 295 K in $CDCl_3$ solution using a Bruker Avance 600 MHz spectrometer. $^1$H and $^{13}$C NMR signals were assigned using two-dimensional $^1$H–$^1$H COSY, $^1$H–$^{13}$C HSQC and $^1$H–$^{13}$C HMBC as well as 1H–1H NOESY spectra. 2D COSY and NOESY spectra were acquired in the magnitude mode with the gradient selection method and with spectral widths of 6562 Hz for both dimensions.

### 3.6. Calculation procedure

Semi-empirical calculations (PM5) of the heat of formation (HOF) and the geometric optimization were performed using the Scigress 2.1.0 program [16]. The DFT calculations were performed using the GAUSSIAN 03 package [17]. The geometries were optimized according to Becke's three parameters hybrid method with the Lee, Yang and Parr correlation functional (B3LYP) [18] and 6-311G(d) basis set. The NMR was calculated using GIAO method in the same base set.

## Acknowledgements

The author thanks the Polish Ministry of Science and Higher Education for financial support under Grants No. NN 204 005536 in the years 2009–2013.

## References

[1] L.D. King, L.M. Safley, J.W. Spears, Agric. Waste 8 (1983) 185–190.
[2] L.R. Chappel, J. Parasitol. 65 (1979) 137–143.
[3] J.W. Westley, C.M. Liu, R.H. Evans Jr., L.H. Sello, N. Troupe, T.J. Hermann, Antibiotic 36 (1983) 1195–1200.
[4] S.C. Gad, C. Reilly, K. Siino, F.A. Gavigan, G. Witz, Toxicology 8 (1985) 451–468.
[5] S.D. Folz, L.H. Nowakowski, B.L. Lee, G.A. Conder, D.L. Rector, T.F. Brodasky, J. Parasitol. 73 (1987) 29–35.
[6] N.B. Logan, M.E. McKenzie, D.P. Conway, L.R. Chappel, N.C. Hammet, Poult. Sci. 72 (1993) 2058–2063.
[7] C.C. Chiang, I.C. Paul, Science 196 (1977) 1441–1443.
[8] P. Malfreyt, Y. Pascal, J.J. Juillard, Chem. Soc. Perkin Trans. 2 (1994) 2031–2038.
[9] J. Ivanova, I.N. Pantcheva, M. Mitewa, S. Simova, M. Tanabe, K. Osakada, Chem. Cent. J. 5 (52) (2011) 1–8.
[10] R. Pankiewicz, D. Remlein-Starosta, G. Schroeder, B. Brzezinski, J. Mol. Struct. 783 (1–3) (2006) 136–144.
[11] R. Pankiewicz, G. Schroeder, B. Gierczyk, G. Wojciechowski, B. Brzezinski, F. Bartl, G. Zundel, Biopolym.: Biospectrosc. 62 (2001) 173–182.
[12] R. Pankiewicz, G. Schroeder, B. Brzezinski, F. Bartl, J. Mol. Struct. 749 (1–3) (2005) 128–137.
[13] F.G. Riddell, S.J. Tompsett, Tetrahedron Lett. 47 (1991) 10109–10118.
[14] A.L. Davis, J.A. Harris, C.A.L. Russell, J.P.G. Wilkins, Analyst 124 (1999) 251–256.
[15] E.F. Paulus, M. Kurz, H. Matter, L.J. Vértesy, Am. Chem. Soc. 120 (1998) 8209–8221.
[16] MO-G Version 1.1, Fujitsu Limited, Tokyo, Japan, 2008.
[17] M.J. Frish, G.W. Trucks, H.B. Schlegel, G. E. Scuseria, M. A. Robb, J. R. Cheeseman, J. A. Montgomery, T. Vreven, K.N. Kudin, J.C. Burant, J. M. Millam, S.S. Iyengar, J. Tomasi, V. Barone, B. Mennucci, M. Cossi, G. Scalmani, N. Rega, G.A. Peterson, H. Nakatsuji, M. Hada, M. Ehara, K. Toyota, R. Fukuda, J. Hasegawa, M. Ishida, T. Nakajama, Y. Honda, O. Kiato, H. Nakai, M. Klene, X. Li, J.E. Knox, H.P. Hratchin, J.B. Cross, C. Adamo, J. Jaramillo, R. Gomperts, R.E. Startmann, O. Yazyev, A.J. Austin, R. Cammi, C. Pomelli, J.W. Octerski, P.Y. Ayala, K. Morokuma, G.A. Voth, P. Salvador, J.J. Dannenbeg, V.G. Zakrzewski, S. Dapprich, A.D. Daniels, M.C. Strain, O. Farks, D.K. Malick, A.D. Rabuck, K. Raghavachari, J.B. Foresman, J.V. Ortiz, Q. Cui, A.G. Baboul, S. Clifford, J. Cioslowski, B.B. Stefanov, G. Liu, A. Liashenko, P. Piskorz, I. Komaromi, R.L. Martin, D.J. Fox, T. Keith, M.A. Al-Laham, C.Y. Peng, A. Nanayakkara, M. Challacombe, P.M.W. Gill, B. Johnson, W. Chen, M.W. Wong, C. Gonzalez, J.A. Pople, Gaussian03, Revision B.04, Gaussian, Inc.: Pittsburgh, PA, 2003.
[18] A. Szwajca, A. Katrusiak, M.J. Szafran, Mol. Struct. 705 (2004) 159–165.